Electronic Supplementary Material (ESI) for RSC Advances.

A new organic NLO material isonicotinamidium picrate (ISPA): Crystal Structure, structural modeling and its physico-chemical properties

RO. MU. Jauhar[a], V. Viswanathan[b], P. Vivek[c], G. Vinitha[d], D. Velmurugan[b], P. Murugakoothan[a*]

[a]MRDL, PG and Research Department of Physics, Pachaiyappa's College, Chennai – 600 030.
[b]Centre of Advanced Study in Crystallography and Biophysics, University of Madras, Guindy Campus, Chennai - 600 025.
[c]Sri Venkateswara Institute of Technology, Kolundhalur, Thiruvallur- 602 001.
[d]Division of Physics, School of Advanced Science, VIT University, Chennai - 600 127.

E-mail: murugakoothan03@yahoo.com

Tel: +91 9444447586

ELECTRONIC SUPPLEMENTARY INFORMATION

Experimental

Material synthesis and crystal growth

Mixed solvents were chosen for the synthesis process because their dependence on temperature enhances the growth rate of the crystals. In such cases, the favourable solvent for the material dominates at higher temperatures and the less favourable one dominates at lower temperatures, thus concentrates on the entire temperature range completely.[1]

When the solute was introduced into the solvent light yellow coloured precipitate was formed and it was dissolved using the same solvent. The resultant product is isonicotinamidium picrate. The schematic chemical reaction is shown in Figure S1. Isonicotinamide is a strong base which accepts a proton in acidic medium and forms the salt of the respective acid. The reaction is a proton transfer reaction where a proton is transferred from the electron donor group of picric acid to the electron acceptor group of isonicotinamide. The solution was stirred continuously for 8 hours to attain homogeneity. The solution was then filtered using Whatman filter paper and

covered with perforated polythene sheet to restrict abundant evaporation. The filtered solution was allowed to evaporate at room temperature (33°C). After a span of 20 days bushy crystals of the title material were harvested.

Then the bushy like crystals were collected, grounded and was used for the solubility studies of the title material. The solubility study was carried out as a function of temperature ranging from 25°C to 45°C with an interval of 5°C using a constant temperature water bath with temperature accuracy of ±0.01°C by gravimetric method. Figure S2 shows the solubility curve of ISPA revealing the positive solubility gradient of the titular material in a 2:1 ratio mixed acetonitrile and water solvent. The solubility of ISPA is found to be 2.9 g/100 mL at 45 °C.

Now with respect to the solubility data, solution was prepared at 45°C, filtered using Whatman filter paper and kept in a constant temperature water bath maintained at 45°C. After a span of 20 days, needle shaped crystals with much improved morphology than those of the crystals grown at room temperature were harvested. But in order to get a better morphology the solution was now prepared at 40 °C as like the procedure mentioned above. After a span of 22 days optical quality crystals were harvested. This can be understood from the fact that evaporation rate and viscosity plays a vital role in the growth of crystals. At 40°C the solution may get suitable solubility with enough evaporation rate associated with optimum viscosity of the solution. When solubility increases, viscosity of the solution also increases, which controls the evaporation rate even at little high temperature and finally growth solution becomes stable. This particular crystal grown at 40°C was used for further characterization studies.

Initially ISPA compound was synthesized using various solvents such as water, methanol, ethanol, acetone and acetonitrile. All these solvents were used to dissolve the ISPA compound separately. But the compound is completely insoluble in all the above solvents. Then

it was tried with mixing ethanol and water, methanol and water, acetonitrile and water in a 1:1 ratio. It was synthesized even by changing the mixed solvents ratio. But, only acetonitrile and water solvent could dissolve the ISPA compound partially. Then, acetonitrile and water were mixed in a 2:1 ratio in which the source materials of the titular compound dissolved completely.

Calculation of polarizability and plasma energy

The valence electron plasma energy $\hbar\omega_P$ is given by,

$$\hbar\omega_P = 28.8\sqrt{\left[\frac{Z\rho}{M}\right]}$$

where Z is the total number of valence electrons, ρ is the density and M is the molecular weight of the ISPA crystal. The plasma energy in terms of Penn gap (E_P) and Fermi gap (E_F) in eV is given as

$$E_P = \frac{\hbar\omega_\rho}{\left(\varepsilon_\infty - 1\right)_{1/2}}$$

and

$$E_F = 0.2948\ \left(\hbar\omega_\rho\right)_{4/3}$$

The polarizability, α, from the Penn gap analysis is given by

$$\alpha = \left\{\frac{\left(\hbar\omega_\rho\right)^2 S_0}{\left(\hbar\omega_\rho\right)^2 S_0 + 3E_P^2}\right\} \text{ x } \frac{M}{\rho} \text{ x } 0.396 \text{ x } 10^{-23}$$

where So is the constant for a particular material and is given by

$$S_0 = 1 - \left[\frac{E_P}{4E_F}\right] + \frac{1}{3}\left[\frac{E_P}{4E_F}\right]^2$$

The value of polarizability α is also be determined using the Clausius–Mossotti relation, which is given as

$$\alpha = \frac{3M}{4\pi N_A \rho}\left(\frac{\varepsilon_\infty - 1}{\varepsilon_\infty + 2}\right)$$

Third order nonlinear optical study

The measurable quantity (ΔTp–v), the difference between the peak and valley transmittances Tp–Tv, as function of on-axis phase shift $|\Delta\Phi_\circ|$ is given by

$$|\Delta\Phi_\circ| = \frac{\Delta T_{P-V}}{0.406(1-S)^{0.25}}$$

where S is the aperture linear transmittance and $|\Delta\Phi_\circ|$ is the on-axis phase shift.

$$S = 1 - \exp\left(\frac{-2r_0^2}{\omega_0^2}\right)$$

The on-axis phase shift is related to the third-order nonlinear refractive index (n_2),

$$n_2 = \frac{\Delta\Phi_0\lambda}{2\pi I_0 L_{eff}}$$

where L_{eff} is the effective thickness of the sample and is given by $L_{eff} = [1-\exp(-\alpha L)]/\alpha$, α is the linear absorption coefficient, L is the thickness of the sample and I_0 is the on-axis irradiance at focus. From open-aperture Z-scan data, the nonlinear absorption coefficient β was estimated using the following relation.

$$\beta = \frac{2\sqrt{2\Delta T}}{I_0 L_{eff}}$$

The real and imaginary parts of the third-order NLO susceptibility $\chi^{(3)}$ were determined from experimental determination of n_2 and β according to the following relations:

$$\text{Re } \chi^{(3)}(\text{esu}) = 10^{-4} \frac{\varepsilon_0 C^2 {n_0}^2 n_2}{\pi} \left(\frac{cm^2}{W}\right)$$

$$\text{Im } \chi^{(3)}(\text{esu}) = 10^{-2} \frac{\varepsilon_0 C^2 {n_0}^2 n_2 \lambda\beta}{4\pi^2} \left(\frac{cm}{W}\right)$$

The absolute value of $\chi^{(3)}$ was calculated from the following relation:

$$|\chi^{(3)}| = \sqrt{\left[\left(Re(\chi^{(3)})\right)^2 + \left(Im(\chi^{(3)})\right)^2\right]}$$

Reference

1 R. Surekha, R. Gunaseelan, P. Sagayaraj and K. Ambujam, *CrystEnggComm*, 2014, 16, 7979.

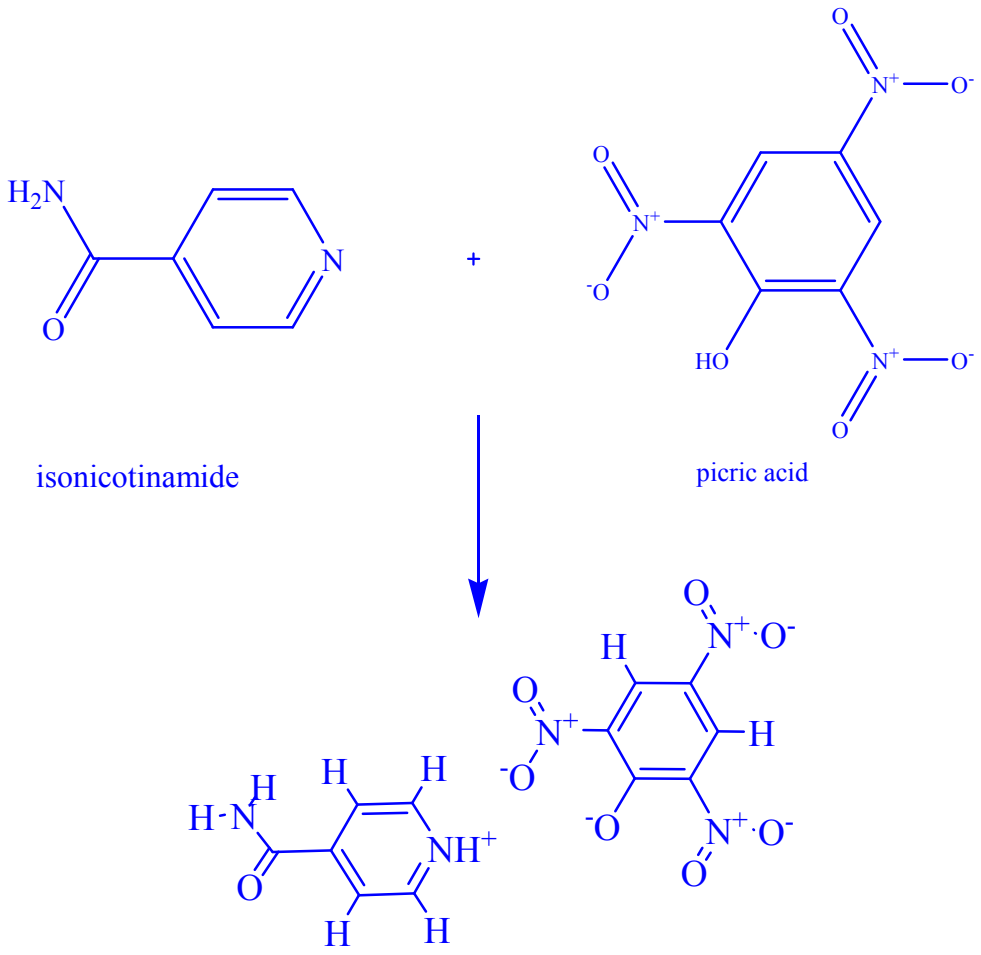

Figure S1 Reaction scheme of ISPA compound

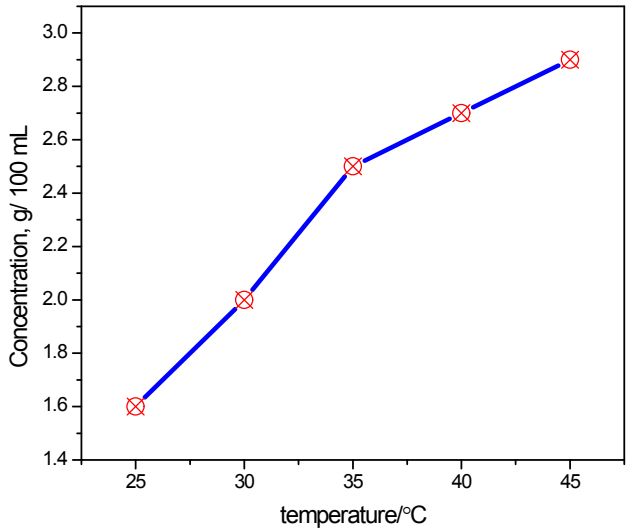

Figure S2 Solubility curve of ISPA

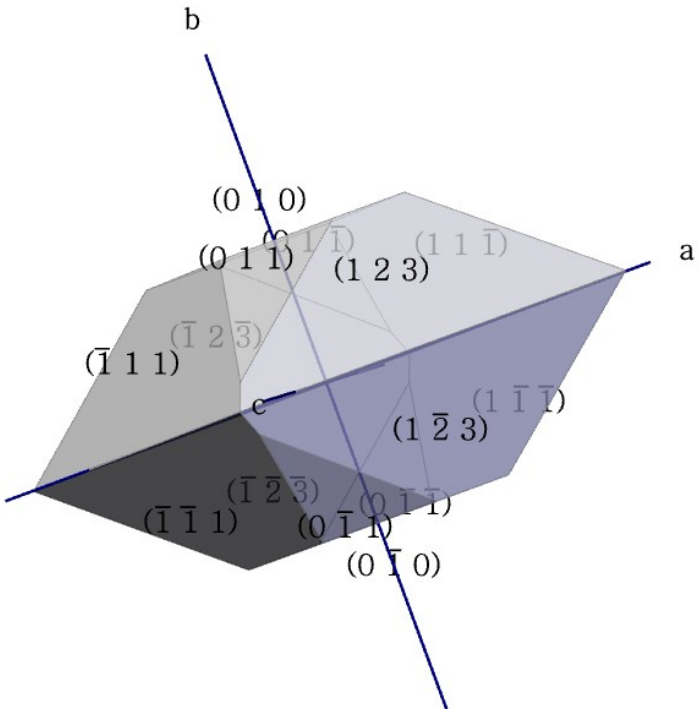

Figure S3 Morphology of ISPA crystal

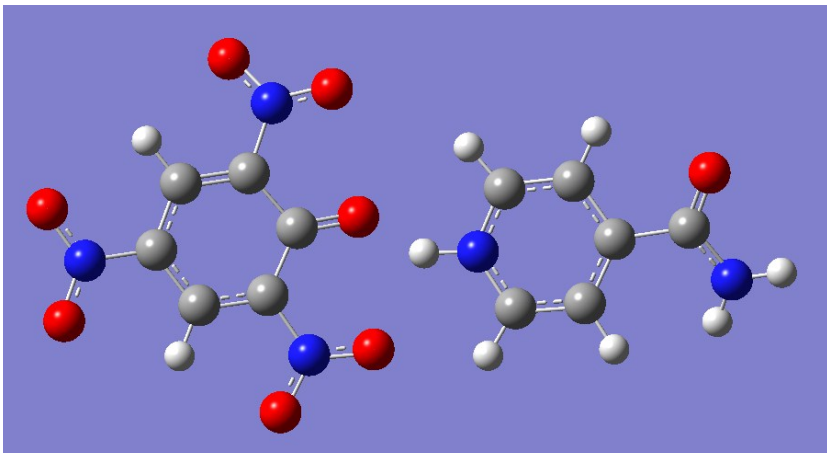

Figure S4 Optimized molecular geometry of ISPA

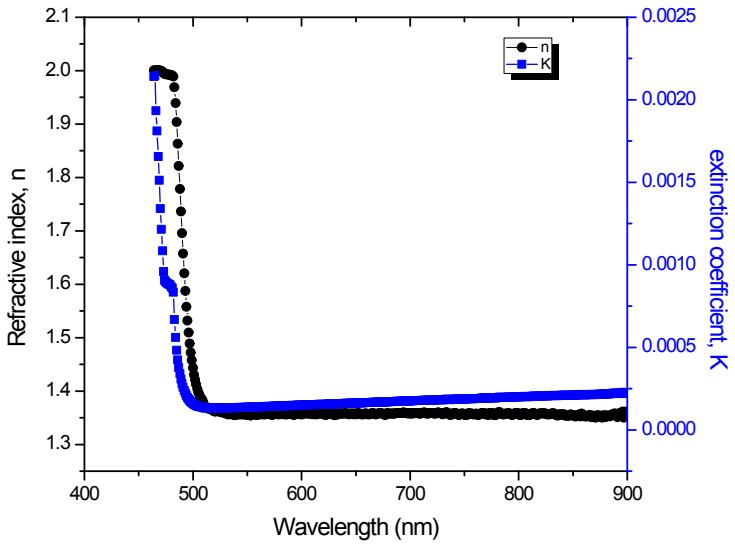

Figure S5 Variation of refractive index and extinction coefficient vs wavelength for ISPA crystal

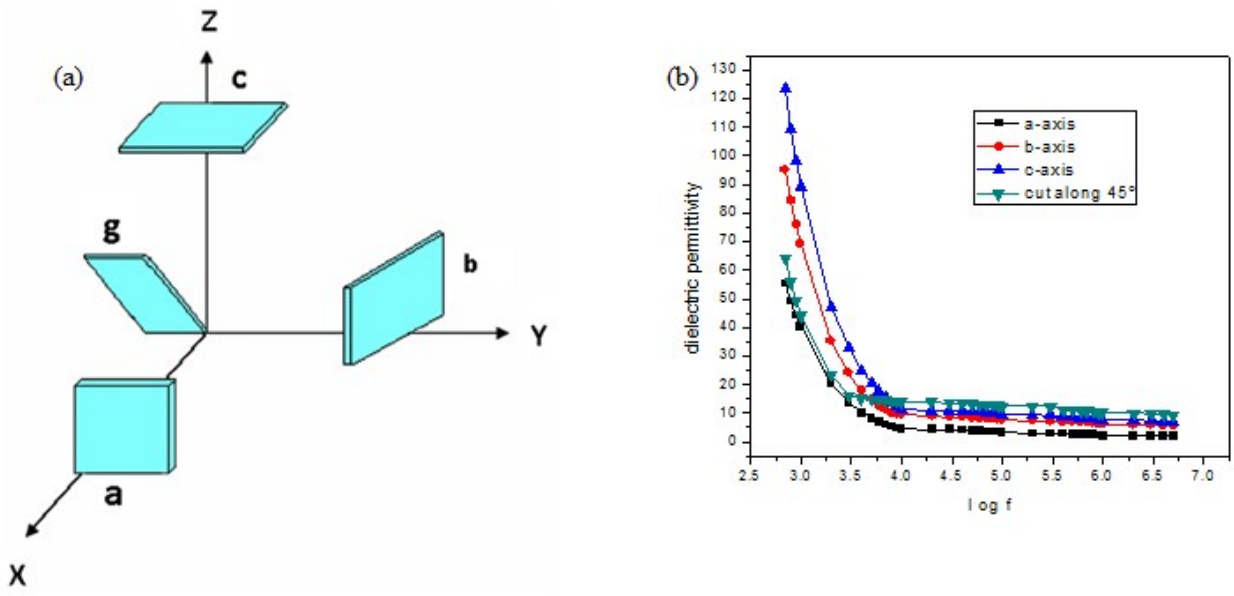

Figure S6 (a) Orientations of the samples for dielectric study

(b) Dielectric tensor components for ISPA crystal

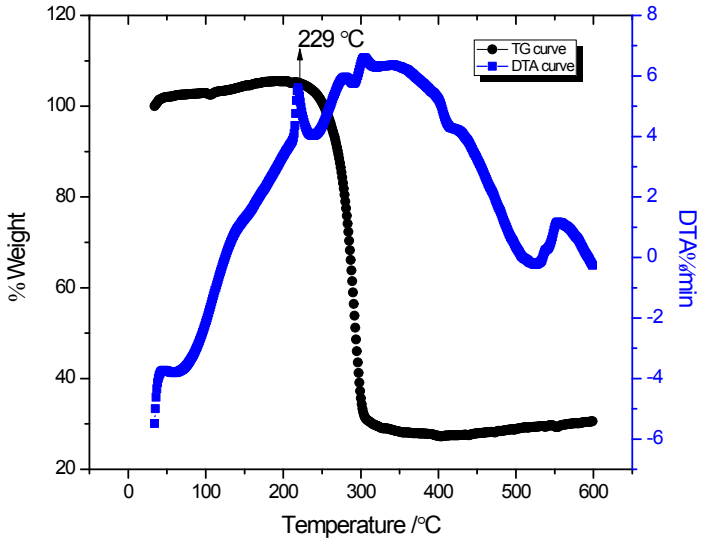

Figure S7 TG-DTA curves of ISPA

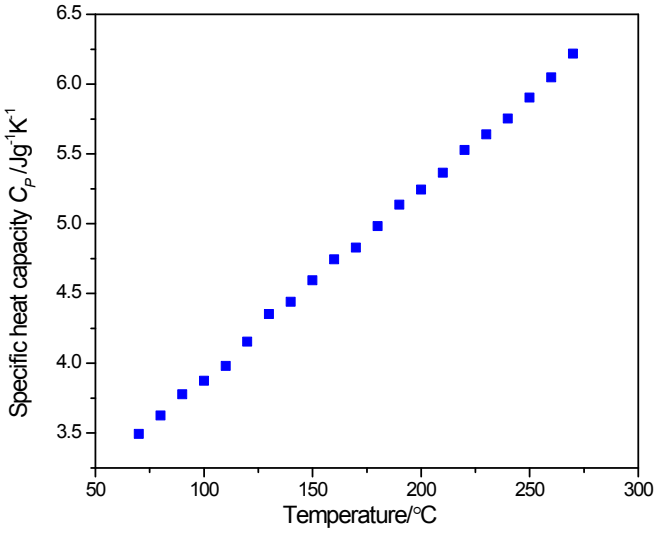

Figure S8 Plot of temperature versus specific heat capacity of ISPA

Table S1 Crystal data and structure refinement for ISPA

Identification code	ISPA
Empirical formula	C_{12} H_9 N_5 O_8
Formula weight	351.24
Temperature	293(2) K
Wavelength	0.71073 Å
Crystal system, space group	monoclinic, $P2_1/n$
Unit cell dimensions	a = 14.290(5) Å, α = 90.000(5)°
	b = 7.430(5) Å, β = 116.638(5)°
	c = 14.697(5) Å γ = 90.000(5)°
Volume ($Å^3$)	1394.8(12)
Z, Calculated density (Mg/m^3)	4, 1.673
Absorption coefficient (mm^{-1})	0.144
F(000)	720
Crystal size (mm^3)	0.20 x 0.15 x 0.10
Theta range for data collection (deg.)	2.68 to 31.47
Limiting indices	-20<=h<=20, -10<=k<=10, -21<=l<=18
Reflections collected / unique[R(int) = 0.0354]	28313 / 4279
Completeness to theta	31.47 92.5 %
Absorption correction	Semi-empirical from equivalents
Max. and min. transmission	0.9858 and 0.9718
Refinement method	Full-matrix least-squares on F^2
Data / restraints / parameters	4279 / 0 / 226
Goodness-of-fit on F^2	1.118
Final R indices [I>2sigma(I)]	R1 = 0.0643, wR2 = 0.1482
R indices (all data)	R1 = 0.1095, wR2 = 0.1711
Largest diff. peak and hole (e $Å^{-3}$)	0.284 and -0.325

Table S2 Selected Bond lengths

Bond length	Experimental (Å)	Theoretical (Å)
O(8)-C(7)	1.244(3)	1.278
N(5)-O(2)	1.208(3)	1.277
N(5)-O(3)	1.229(3)	1.267
N(5)-C(12)	1.456(3)	1.443
O(1)-C(6)	1.217(3)	1.248
N(2)-C(6)	1.322(3)	1.363
C(3)-C(6)	1.512(3)	1.507
N(1)-C(1)	1.333(3)	1.354
N(1)-C(5)	1.335(3)	1.349
N(4)-O(4)	1.215(3)	1.267
N(4)-O(5)	1.225(3)	1.267
N(4)-C(10)	1.444(3)	1.449
N(3)-O(7)	1.211(3)	1.264
N(3)-O(6)	1.220(3)	1.269
N(3)-C(8)	1.447(3)	1.458
O(2)-N(5)-O(3)	122.8(2)	121.6
O(2)-N(5)-C(12)	120.1(2)	119.5
O(3)-N(5)-C(12)	117.1(2)	118.7
C(1)-N(1)-C(5)	122.6(2)	122.8
C(11)-C(12)-N(5)	116.51(19)	116.5
C(7)-C(12)-N(5)	118.47(18)	120.8

O(8)-C(7)-C(8)	125.3(2)	124.5
O(8)-C(7)-C(12)	123.20(19)	121.4
O(4)-N(4)-O(5)	122.4(2)	123.8
O(4)-N(4)-C(10)	118.97(19)	118.1
O(5)-N(4)-C(10)	118.64(19)	117.9
O(1)-C(6)-N(2)	123.6(2)	122.7
O(1)-C(6)-C(3)	118.9(2)	120.0
N(2)-C(6)-C(3)	117.5(2)	117.2
O(7)-N(3)-O(6)	122.0(2)	123.2
O(7)-N(3)-C(8)	120.0(2)	119.3
O(6)-N(3)-C(8)	117.9(2)	117.2
C(9)-C(10)-N(4)	118.87(19)	119.3
C(11)-C(10)-N(4)	119.58(19)	119.4
C(9)-C(8)-N(3)	116.04(19)	116.8
N(3)-C(8)-C(7)	119.60(19)	119.9
N(1)-C(1)-C(2)	119.8(2)	119.6
N(1)-C(5)-C(4)	119.4(2)	119.5

Table S3 Selected Torsion angles

Bond	Bond angle (°)
O(2)-N(5)-C(12)-C(11)	146.3(2)
O(3)-N(5)-C(12)-C(7)	144.7(2)
N(5)-C(12)-C(11)-C(10)	179.1(2)
C(11)-C(12)-C(7)-O(8)	179.5(2)
N(5)-C(12)-C(7)-C(8)	-176.70(19)
C(2)-C(3)-C(6)-O(1)	-163.2(2)
C(4)-C(3)-C(6)-N(2)	-168.6(2)
C(12)-C(11)-C(10)-N(4)	179.2(2)
O(4)-N(4)-C(10)-C(9)	179.3(2)
O(5)-N(4)-C(10)-C(11)	176.7(2)
O(7)-N(3)-C(8)-C(9)	-159.0(2)
O(6)-N(3)-C(8)-C(7)	-155.6(3)
O(8)-C(7)-C(8)-C(9)	-179.8(2)
C(12)-C(7)-C(8)-N(3)	175.5(2)
N(3)-C(8)-C(9)-C(10)	-177.5(2)
N(4)-C(10)-C(9)-C(8)	-179.6(2)

Table S4 Hydrogen Bonds

D—H…A	D—H(Å)	H…A(Å)	D…A(Å)	D—H…A[°]
N(1)-H(1A)…O(7) [i]	0.86	2.18	2.8457(19)	134
N(1)-H(1A)…O(8) [i]	0.86	1.91	2.6551(18)	144
N(2)-H(2A)…O(4) [ii]	0.86	2.51	3.239(2)	143
N(2)-H(2A)…O(5) [ii]	0.86	2.39	3.222(2)	164
N(2)-H(2B)…O(3) [iii]	0.86	2.21	3.026(2)	159
C(1)-H(1)…O(6) [iv]	0.93	2.34	3.048(2)	133
C(5)-H(5)…O(7) [i]	0.93	2.56	3.037(2)	112
C(5)-H(5)…O(5) [v]	0.93	2.59	3.410(2)	148
C(11)-H(11)…O(1) [vi]	0.93	2.42	3.304(2)	159

Symmetry codes: i) -x,-y,1-z; ii) -x,1-y,-z; iii) -1/2+x,1/2-y,-1/2+z; iv) -1/2-x,-1/2+y,1/2-z; v) 1/2+x,1/2-y,1/2+z; vi) 1/2-x,1/2+y,1/2-z.

Table S5 Parameters for Polarizability

Parameter	Values
Plasma Energy (eV)	22.664
Penn gap (eV)	7.554
Fermi gap (eV)	18.710
Polarizability (cm^{-3}) Penn analysis	6.0583×10^{-23}
Claussius Mossotti (cm^{-3}) equation	6.24×10^{-23}